JPn Neuroscience

The Journal of Physiology

J Physiol 592.1 (2014) pp 203–214

Velocity storage mechanism in zebrafish larvae

Chien-Cheng Chen[1,4], Christopher J. Bockisch[1,2,3], Giovanni Bertolini[1], Itsaso Olasagasti[1], Stephan C. F. Neuhauss[5,6,7], Konrad P. Weber[1,2], Dominik Straumann[1,6,7] and Melody Ying-Yu Huang[1,6,7]

Departments of [1]Neurology, [2]Ophthalmology and [3]Otorhinolaryngology, University Hospital Zurich, CH-8091, Zurich, Switzerland
[4]PhD Program in Integrative Molecular Medicine, Life Science Graduate School, CH-8057, Zurich, Switzerland
[5]Institute of Molecular Life Sciences, University of Zurich, CH-8057, Zurich, Switzerland
[6]Zurich Center for Integrative Human Physiology (ZIHP), CH-8057, Zurich, Switzerland
[7]Neuroscience Center Zurich (ZNZ), CH-8057, Zurich, Switzerland

Key points

- Five-day-old zebrafish larvae already exhibit a velocity storage mechanism (VSM).
- The VSM in zebrafish larvae emerges earlier than a functional horizontal angular vestibular reflex.
- The VSM may be critical to ocular motor control in larval zebrafish.

Abstract The optokinetic reflex (OKR) and the angular vestibulo-ocular reflex (aVOR) complement each other to stabilize images on the retina despite self- or world motion, a joint mechanism that is critical for effective vision. It is currently hypothesized that signals from both systems integrate, in a mathematical sense, in a network of neurons operating as a velocity storage mechanism (VSM). When exposed to a rotating visual surround, subjects display the OKR, slow following eye movements frequently interrupted by fast resetting eye movements. Subsequent to light-off during optokinetic stimulation, eye movements do not stop abruptly, but decay slowly, a phenomenon referred to as the optokinetic after-response (OKAR). The OKAR is most likely generated by the VSM. In this study, we observed the OKAR in developing larval zebrafish before the horizontal aVOR emerged. Our results suggest that the VSM develops prior to and without the need for a functional aVOR. It may be critical to ocular motor control in early development as it increases the efficiency of the OKR.

(Received 10 May 2013; accepted after revision 4 November 2013; first published online 11 November 2013)
Corresponding authors M. Ying-Yu Huang or D. Straumann: Neurology Department, University Hospital Zurich, Frauenklinikstrasse 26, CH-8091 Zurich, Switzerland. Email: ying-yu.huang@usz.ch or dominik.straumann@usz.ch

Abbreviations aVOR, angular vestibulo-ocular reflex; dpf, days post-fertilization; N–T, nasal-to-temporal; OKAN, optokinetic after-nystagmus; OKAR, optokinetic after-response; OKR, optokinetic response; ROI, region of interest; T–N, temporal-to-nasal; VPNI, velocity-to-position neural integrator; VSM, velocity storage mechanism.

Introduction

The optokinetic response (OKR) is a visually guided ocular motor reflex evoked by the moving surround primarily during self-motion. Via a neuronal network operating as a velocity storage mechanism (VSM), the optokinetic reflex (OKR) and the vestibulo-ocular reflex (VOR) work in concert to ensure gaze stability, being critical for effective vision (Baaarsma & Collewijn, 1974; Robinson, 1981; Paige, 1983; Schweigart *et al.* 1997). The OKR consists of slow-phase eye movements that stabilize images of the moving scene on the retina and oppositely directed fast phases that reset the position of the eyes. The OKR has been extensively studied in species with fovea, such as monkeys (Takahashi & Igarashi, 1977; Igarashi *et al.* 1977) and humans (Honrubia *et al.* 1968; Abadi & Pantazidou, 1997), and without fovea, such as rabbits (Tan *et al.* 1992, 1993), rats (Sirkin *et al.* 1985; Hess *et al.* 1985) and goldfish (Beck *et al.* 2004). Interestingly, after the OKR reaches a steady state during optokinetic stimulation with constant velocity, the nystagmus continues during subsequent total darkness and its slow phase eye velocity decreases exponentially. This exponentially decaying eye velocity is called the optokinetic after-response (OKAR).

DOI: 10.1113/jphysiol.2013.258640

The OKAR is thought to be the result of the VSM that is probably shared with the vestibular system (Cohen *et al.* 1977; Raphan *et al.* 1977, 1979; Robinson, 1977). The VSM can be charged either by the eye velocity signal of the OKR or by the angular velocity signal of the angular VOR (aVOR). The aVOR is evoked by head rotation and generates eye movements in the opposite direction of the head movement to keep the visual world stable on the retina. At present, it is suggested that the VSM exercises its effect via integration of visual information with vestibular inflow in the central vestibular pathway, which also merges different sensory input information (e.g. semicircular canals, otoliths, visual system, neck proprioception, etc.) to better estimate body motion critical for synchronizing motor output required for eye/body stabilization (Angelaki & Cullen, 2008). The existence of a VSM can explain how low-frequency signals from the semicircular canals are perseverated (Robinson, 1977; Raphan *et al.* 1977, 1979). In addition, it has been shown that the VSM also integrates OKR velocity signals, which can explain the phenomenon of the OKAR (Waespe & Henn, 1977; Raphan *et al.* 1979; Cohen *et al.* 1981). Since the OKAR is eliminated after bilateral labyrinthectomy (Uemura & Cohen, 1973; Zee *et al.* 1976; Collewijn, 1976), it is conceivable that signals from the semicircular canals are essential for the VSM. However, in small vertebrate animals such as larval teleost fish and *Xenopus*, it has been shown that the aVOR emerges later than the OKR, which is due to the tiny semicircular canals being too small to be functional (Beck *et al.* 2004; Lambert *et al.* 2008). Given the observation that the VSM subserves both the vestibular and optokinetic systems, and given the importance of the OKR in the visual system of afoveated animals such as teleost fish, we question whether the development of the VSM requires the behavioural onset of the aVOR. To find out whether the VSM exists before the aVOR is functional, we tested zebrafish larvae at 5–6 days post fertilization (dpf). At this stage the zebrafish OKR is fully functional, but the horizontal aVOR is not yet developed (Beck *et al.* 2004; Mo *et al.* 2010). One previous study reported that the OKAR in zebrafish larvae does not yet exist as eye velocity elicited by optokinetic stimulation immediately dropped to zero after switching the lights off (Beck *et al.* 2004). However, the measured eye velocity does not represent the velocity command from the velocity storage, as the latter is integrated by the velocity-to-position neural integrator (VPNI), which in zebrafish larva is very leaky (Miri *et al.* 2011), before reaching the eye muscle. The leakiness of the integrator causes an almost immediate drop and a reversal of the eye velocity during OKAR, causing the eyes to rapidly return to the resting position, masking the effect of a putative VSM (Ramat & Bertolini, 2009). Therefore, using a single exponential function to analyse the velocity drop after the OKR, as Beck *et al.* have done, would underestimate the time constant of the velocity decay. Such a method is neither sufficient nor conclusive. We re-addressed the question of the VSM in zebrafish larvae by focusing on post-optokinetic ocular drift in the position domain, which allowed us to take into account the effect of the individual VPNI time constant of each larva.

Methods

Fish maintenance and breeding

Wild-type zebrafish, WIK strain, were bred and maintained as described previously (Mullins *et al.* 1994). Embryos were raised under a standard 10 h dark/14 h light cycle at 28°C in E3 medium (5 mM NaCl, 0.17 mM KCl, 0.33 mM $CaCl_2$, and 0.33 mM $MgSO_4$) (Haffter *et al.* 1996) and staged according to development in days post-fertilization (dpf). Ten larvae were tested.

Optokinetic stimulation

A schematic drawing of the setup is shown in Fig. 1*A* and *B*. Using four digital light projectors (Samsung SP-H03 Pico Projector), moving and stationary vertical sine-wave gratings with 100% contrast (maximum illumination 1524 lux) and spatial frequency of 0.056 cycles deg^{-1} were projected onto a translucent screen wrapped around a glass cylinder at an angular velocity of 0, 10, or 20 deg s^{-1}. Moreover, four shutters were used to block the light sources of the projectors to create a totally dark environment. Data acquisition, properties of the visual

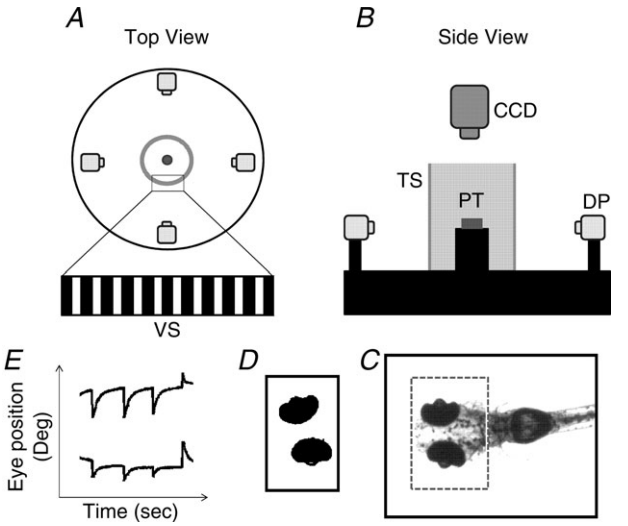

Figure 1. Schematic diagram of the experimental setup and the image analysis process
Top view (*A*) and side view (*B*) of the experimental setup. *C*, recorded image of the whole body of the larval zebrafish. The dashed square indicates the ROI. *D*, the eye balls were identified and analysed to obtain eye movements. *E*, eye movement in space. DP, digital projector; CCD, IR-sensitive CCD camera; TS, translucent screen; VS, visual stimulus; PT, plastic tube.

stimulation, and light source switches were all controlled by custom-made programs written in LabVIEW 10.0 (National Instruments, USA) and Borland Delphi 7.0 (Borland Software Corporation, USA).

Recording of eye/body movements

Ten larvae at 5–6 dpf were randomly chosen from a single clutch and tested individually. In order to suppress whole-body motion without constricting eye movements, single larvae were embedded dorsal side up in the centre of a 21 mm transparent plastic tube containing 3–3.5% methylcellulose. The embedded larva was placed inside the cylinder at a distance of the larva's eye to the screen of approximately 6.8 cm and was illuminated from below with infrared (IR)-emitting diodes ($\lambda_{peak} = 875 \pm 15$ nm, OIS-150 880, OSA Opto Light GmbH, Germany). During binocular stimulation, movements of both eyes were recorded by an IR-sensitive charge-couple device (CCD) camera with a sample rate of 40 frames s^{-1}. Frames were processed by custom-developed software (LabVIEW 10.0; National Instruments, USA). Before the recording began, a region of interest (ROI) was manually selected around the eyes (Fig. 1*C*). Based on the pigmentation the software extracted the ellipse-like shape of the eye from the ROI by applying binary threshold and a filter to delete small particles until both eyes could be clearly identified (Fig. 1*D*). Angular eye position was calculated based on the centre of mass and the axis with the lowest angular momentum of each eye and was plotted against time (Fig. 1*E*). Both image recording and analysis of eye position were achieved in real-time and were monitored during the experiment on the computer. For the subsequent off-line analysis of the eye movement relative to the body, every frame was saved during on-line recording. The larval body movement was analysed by calculating the body axis in each frame with a similar image-processing algorithm as applied in on-line eye recognition. The code for calculating the body axis was written in MATLAB (Mathworks, Natick, MA, USA).

Experimental procedure

Spontaneous eye movements in the dark were recorded for 10 min in each larva. Subsequently, a series of OKR/OKAR tests were performed. The angular velocity of the optokinetic stimulus was the independent variable in the OKR/OKAR test, having four levels (-10, $+10$, -20, $+20$ deg s^{-1}). A single OKR/OKAR test consisted of 30 s of stationary gratings presented to the tested larva, followed by 30 s of vertical gratings rotating at a constant angular velocity, and finally, 30 s of darkness. For each stimulus velocity, the OKR/OKAR test was repeated five times. Hence, a total of 20 OKR/OKAR tests (four stimulus velocities repeated five times) were applied to each larva. All larvae were recorded binocularly and data from both eyes were collected for further analysis.

Data analysis and iterative fitting procedure

Data analysis was done by a custom-developed program written in MATLAB (Mathworks). Eye position traces were smoothed using a Gaussian filter with cutoff frequency of 5.5 Hz. Eye velocity was computed as the derivative of eye position. The OKR gain was computed as the maximal slow phase velocity divided by the image velocity. The overall OKR gain was calculated by averaging the OKR gain across trials. The time constants of VPNI were estimated by fitting a single exponential curve to position traces of spontaneous eye movements recorded in darkness (for details, see Results and Fig. 2). The VSM time constant was estimated fitting the following equation to the eye position recorded in darkness after optokinetic stimulation:

$$x(t) = (x_0 - \text{offset})e^{\frac{-t}{T_{NI}}} + \text{offset} + \text{Amp}\left[1 \Big/ \left(\frac{1}{T_{VS}} - \frac{1}{T_{NI}}\right)\right]\left(e^{\frac{-t}{T_{NI}}} - e^{\frac{-t}{T_{VS}}}\right) \quad (1)$$

where t is time, x is eye position, x_0 is the initial eye position, 'offset' is the eye position at the end of the decay, T_{NI} is the time constant of the VPNI, T_{VS} is the time constant of the VSM, and 'Amp' is the amplitude of the VSM output. Equation (1) represents the combination of two terms. The first term describes the decay from an eccentric eye position in the absence of additional velocity input, i.e. a spontaneous eye drift in the dark. The second term describes the convolutional effect of the VSM and the VPNI, i.e. the VPNI receiving post-optokinetic velocity input from the VSM.

Statistical analysis

In order to test for directional preference in the VPNI and the VSM, we compared the following two categories using a binomial test: 'median time constant in temporal-to-nasal (T–N) direction is greater than that in nasal-to-temporal (N–T) direction' or 'median time constant in N–T direction is greater than that in T–N direction'. Since eye movements of both eyes are yoked, T–N movement of one eye co-occurs with N–T movement of the other eye and vice versa. Hence, we compared median time constant of T–N movement of the left eye with that of N–T movement of the right eye and vice versa across subjects.

One larva showed no movement of the left eye in T–N direction (and consequently, no movement of the right eye in N–T direction). We therefore excluded its eye movement in that direction from the tests.

Results

Gaze stability in the dark

Zebrafish larvae showed stable eye positions in the light, when the visual surround is structured (Fig. 2*A*, middle). In the dark, however, the eyes drifted centripetally after each saccade (Fig. 2*A*, left, and *B*). Thus, it appears that the velocity-to-position neural integrator (VPNI) in zebrafish larvae is rather leaky, which in the light is compensated by the optokinetic system, keeping gaze stable (Fig. 2*A*, middle). We characterized the VPNI by a single-exponential fit to each intersaccadic segment of eye position as a function of time (Fig. 2*C*). The mean (±SD) VPNI time constants with initial positions in the temporal and the nasal hemifields of gaze were 3.8 ± 2.1 s and 1.9 ± 0.7 s, respectively, for the left eye, and 3.7 ± 1.9 s and 2.6 ± 1.5 s, respectively, for the right eye. Values of individual zebrafish are depicted in Fig. 2*D* for visual comparison. Note there was one larva that only displayed movements of the left eye in nasal-to-temporal (N–T) direction during the 10 min dark period. Therefore, two data points were absent. There are 38 data points shown in Fig. 2*D* (9 larvae with four data points and one larva with only two data points). Using a binomial test, we found that centripetal eye drifts from temporal initial positions had longer time constants than centripetal eye drifts from nasal initial positions, $n = 19$, $Z = 3.44$, $P = 0.0003$. Whether these differences reflect mechanical properties of the eye plant or have a neural origin is still open to question.

Optokinetic response (OKR)

In 5- to 6-day-old zebrafish larvae, generally, the OKR was initially efficient and the slow phase eye velocity was able to nearly reach its maximal value within 2 s after OKR onset. Subsequently, the slow phase eye velocity slowly decreased despite continuing optokinetic simulation with constant velocity (see typical example in Fig. 3). As a result, a difference between the maximum slow phase eye velocity and the median eye velocity was observed. On average, the maximum slow phase eye velocity was 9.3 ± 0.7 deg s^{-1} at a stimulus velocity of 10 deg s^{-1} and 14.6 ± 1.6 deg s^{-1} at a stimulus velocity of 20 deg s^{-1} while the median eye velocity of the 30 s optokinetic stimulation was 5.2 ± 1.0 deg s^{-1} at a stimulus velocity of 10 deg s^{-1} and around 5.7 ± 1.5 deg s^{-1} at a stimulus velocity of 20 deg s^{-1}. Additionally, the beating field during the OKR shifted in the direction of slow phases. On average, the difference between the mean eye position during the first 10 s and the last 10 s was 9.3 ± 2.4 deg at a stimulus velocity of 10 deg s^{-1} and 7.8 ± 1.4 deg at a stimulus velocity of 20 deg s^{-1}.

Optokinetic after-response (OKAR)

Usually, no saccadic eye movement could be detected immediately after the lights were switched off during optokinetic stimulation, i.e. no nystagmus was found during this time period (Fig. 4). The majority of eye position traces returned toward a more central eye position, which was in the opposite direction to the preceding OKR slow phase. As a result, eye velocity quickly dropped to zero and crossed the zero line (see arrows in Fig. 3*B* and *D*). Specifically, when the initial position was eccentric toward the OKR beating field at light-off, the eyes drifted directly toward the centre (Fig. 4*B*, upper three traces, and *D*, blue trace). However, if the initial eye position was close to the central eye position at light-off, the eyes typically continued moving in the direction of previous OKR slow phases, before turning around to drift toward the centre (Fig. 4*B*, lowest cyan trace, and *D*, green and red traces).

If there was no after-effect of the OKR during the subsequent period in the dark, the eyes would drift exponentially toward the centre with the time constant of the VPNI. However, we found that some post-optokinetic ocular drifts first continue in the direction of the previous OKR slow phases (see again in Fig. 4), suggesting the presence of an optokinetic after-effect visible at least in the position domain. To quantify this observation and verify the physiological meaning of these peculiar eye traces, we decided to compare spontaneous eye drifts in the dark with eye drifts in the dark after optokinetic stimulation. Differences between the eye drifts in these two conditions would indicate an optokinetic after-effect, e.g. due to the velocity storage mechanism (VSM).

Simulation of OKAR with a leaky VPNI

To illustrate our hypothesis, namely that the difference between post-OKR and spontaneous eye drifts in the dark is due to the VSM, we first show the results of a simulation. A conceptual ocular motor model of zebrafish larvae is depicted in Fig. 5*A*. The optokinetic system receives visual input and transmits velocity signals to the VPNI, which integrates the signals to position commands. This pathway is represented with continuous lines. If the VSM exists, it will be charged by the velocity signals from the optokinetic system and then releases the velocity signals to the VPNI as shown with dashed lines. We then modelled spontaneous eye drifts in the dark with a single time constant representing a leaky integrator (Fig. 5*B*). With zero velocity input (e.g. when the OKR is inactive such as in darkness), eye position traces decay exponentially from eccentric positions reached by a saccade (Fig. 5*C*). However, if the input to the leaky VPNI is an exponentially decaying velocity signal, representing the perseverated optokinetic signal in the dark, i.e. stored velocity by leaky

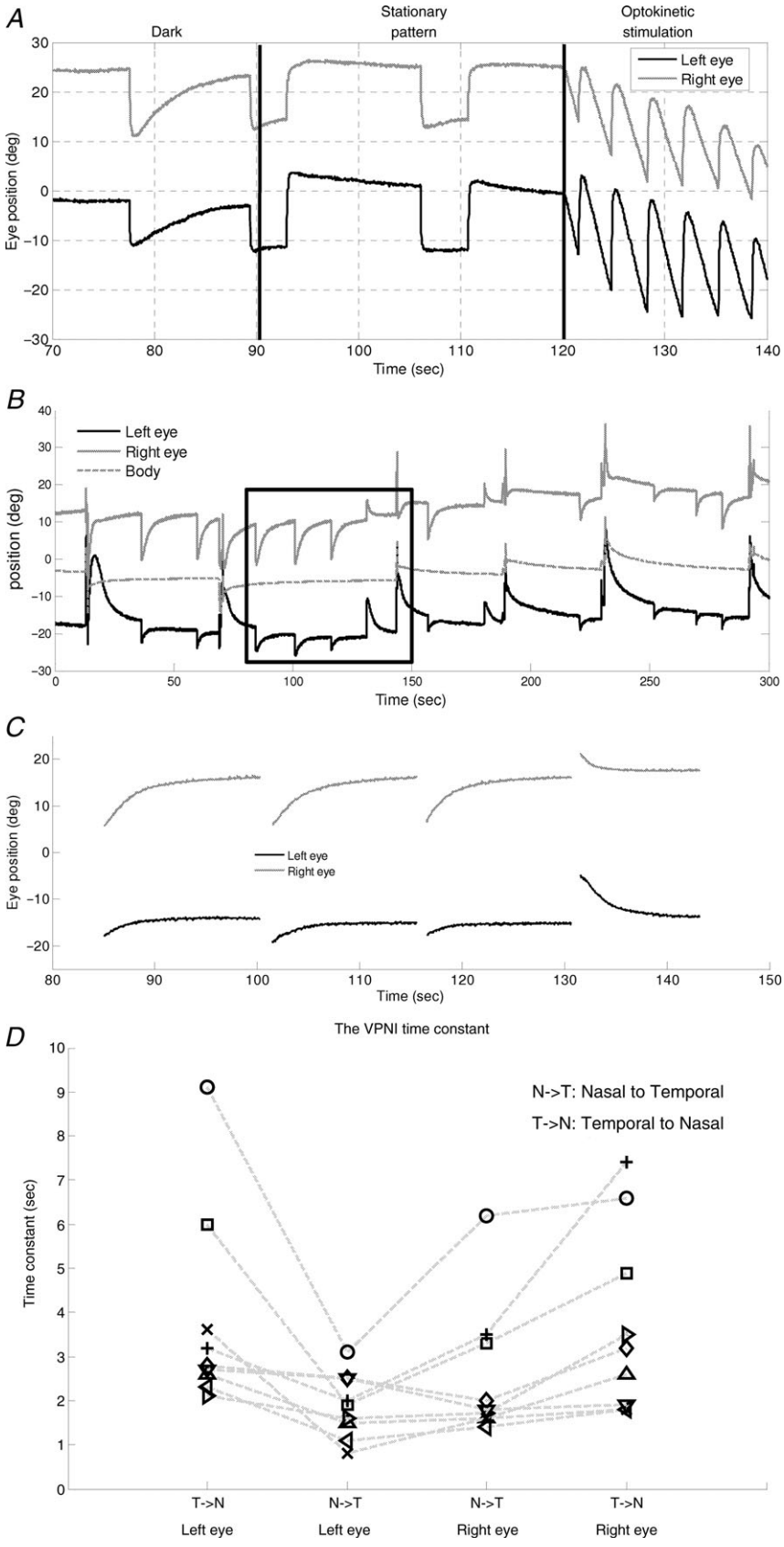

Figure 2. Eye movements of a zebrafish larva under various visual conditions and estimation of time constant of the VPNI
A, eye movements under various visual surrounds. *B*, spontaneous eye drifts in the dark. The body position trace (dotted line) was used to obtain the eye position relative to body axis. *C*, after filtering out saccades and body movements, spontaneous eye drifts were split into segments for applying a single exponential decay curve fitting to estimate the VPNI time constant. *D*, the median time constants of the VPNI of all larvae ($n = 10$). Note there was one larva that only showed movements of the left eye in N–T during the 10 min dark period. Therefore, nine larvae have four values indicating the median time constant of two eyes in two directions, while one larva only has two values indicating the median time constant of two eyes in one direction. The two values are not connected by any line. Values of each fish are connected by a dashed line.

integration, we obtain curves resembling the post-OKR eye drifts recorded in zebrafish larvae (compare Fig. 5*D* to Fig. 4*B*). Specifically, eye drifts from initial positions close to the centre position continued their path in the direction of the velocity signal before drifting toward the centre (Fig. 5*D*, lower traces). In contrast, eye drifts from initial positions eccentrically displaced in the direction of the velocity signal decay immediately toward the centre position (Fig. 5*D*, upper traces).

Estimation of VSM time constant

The simulated examples illustrate the difference between post-OKR eye drifts with and without a VSM. In a second step, we used a model including the VSM and the VPNI to compute the time constant of the VSM for every measured post-OKR eye drift.

Specifically, in a given zebrafish larva, we selected its post-OKR eye drifts that decayed to a stable centre position

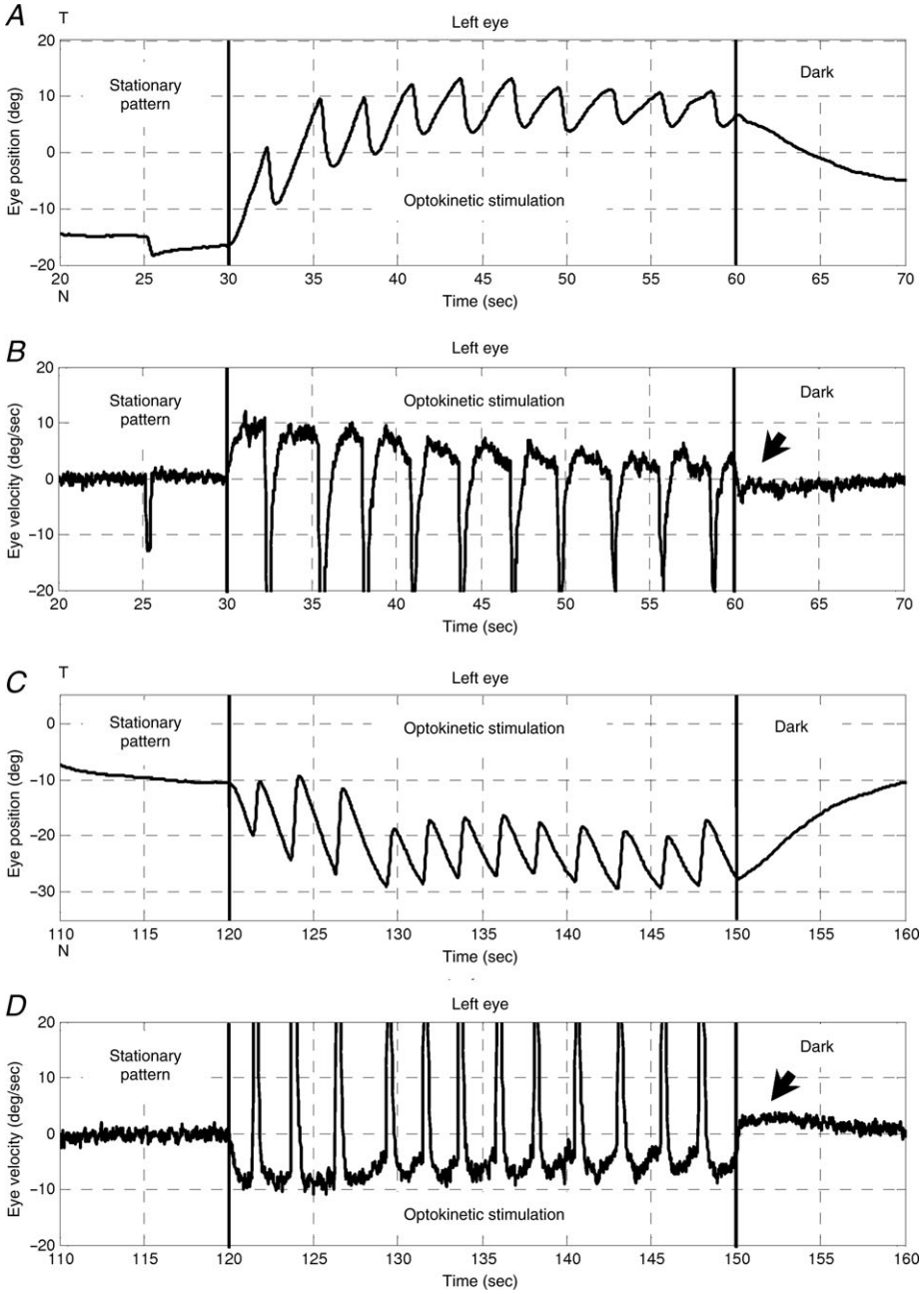

Figure 3. OKR of a zebrafish larva
Optokinetic stimulation was 10 deg s^{-1} in the nasal-to-temporal direction (30–60 s) and 10 deg s^{-1} in the temporal-to-nasal direction (120–150 s). *A* and *C*, left eye position *versus* time. *B* and *D*, left eye velocity *versus* time. Arrows indicate the OKAR in the velocity domain. T, temporal; N, nasal.

without saccadic interruption (e.g. traces in Fig. 4*B*). The contribution of the VSM is obtained by subtracting the eye position drift, as calculated using the time constant of the VPNI (as determined from spontaneous eye drifts in the dark, Fig. 2*D*) and the initial and final position of the selected trace, from the measured post-optokinetic eye position trace (Fig. 6*A*). Then iterative fitting with eqn (1), which was obtained by convolution of VSM and VPNI effects, was applied on these selected traces to estimate the time constant of the VSM (see Methods). The mean VSM time constants of the right and the left eye in all zebrafish larvae tested were 2.0 ± 1.0 s and 1.8 ± 0.8 s, respectively. Data points from individual zebrafish are depicted in Fig. 6*B*. As expected, a binomial test result indicated that

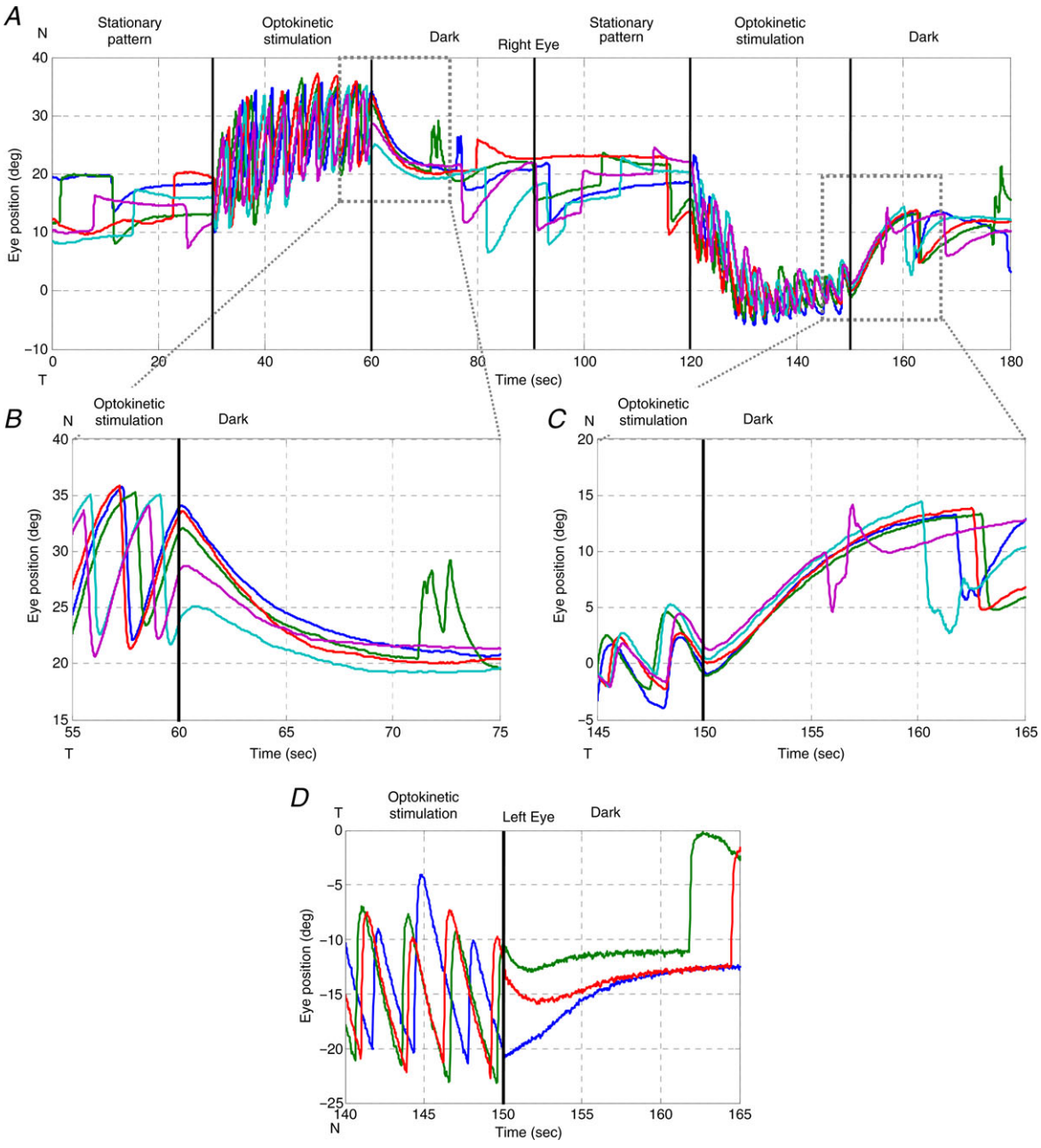

Figure 4. OKAR of a zebrafish larva
Visual stimuli over time: 0–30 s, stationary vertical gratings; 30–60 s, vertical gratings rotating horizontally at a constant angular velocity of 10 deg s^{-1} in one direction; 60–90 s, dark period. At 90–180 s, the same procedure was repeated with the optokinetic stimulus moving in the opposite direction (120–150 s). Different colours indicate different trials. *A*, typical eye position trace of a larval zebrafish during the OKR and OKAR tests. *B* and *C*, magnifications of Fig. 4*A*. *D*, another example of OKAR. The green and red lines indicate that OKAR continued in the direction of the OKR for 2–3 s while the blue line turned to the opposite direction immediately.

the VSM time constant was relatively independent of initial eye position ($n = 19$, $Z = -0.9425$, $P = 0.8265$), which is in contrast to the VPNI time constant that showed a nasal–temporal difference ($n = 19$, $Z = 3.44$, $P = 0.0003$, see Fig. 2*D*).

Discussion

We found the first evidence in zebrafish larvae for the existence of a velocity storage mechanism (VSM) at 5–6 days post-fertilization (dpf). At this early stage, the horizontal angular vestibulo-ocular response (aVOR) is not yet developed (Beck *et al.* 2004; Mo *et al.* 2010) while the optokinetic response (OKR) is already fully functional in 4 dpf larvae (Easter & Nicola, 1997; Huang & Neuhauss, 2008). The display of an optokinetic after-response (OKAR), identifiable through the slower decay of post-optokinetic eye drifts (Fig. 6*A*, black line) compared to that of spontaneous eye drifts in the dark (Fig. 6*A*, grey line), indicates the existence of a VSM (Fig. 6*A*, dotted line).

The very short time constant of the velocity-to-position neural integrator (VPNI) in zebrafish larvae (on average 3–4 s), could explain why Beck *et al.* (2004) did not find evidence for an OKAR of zebrafish larvae in the velocity domain. A simple derivative, as is commonly used to obtain eye velocity, does not, in fact, reproduce the pure VSM signal, but a velocity signal which fades away very quickly, due to the effect of the leaky VPNI. The simulations in Fig. 7 show the difference between the output of a VSM model with a time constant of 2 s and the derivative of the position signal obtained by processing such output through a VPNI with a time constant of 4 s. A single exponential fit to the latter will underestimate the time constant of the VSM to 0.99 s suggesting that no storage function exists.

The function of the VPNI is to convert eye velocity signals (e.g. from saccadic burst neurons) into eye position commands. This is required to keep gaze stable at the new position against the elastic forces of the extra-ocular tissues that pull the eyes toward a central position (Robinson, 1964; Cohen & Komatsuzaki, 1972; Skavenski & Robinson,

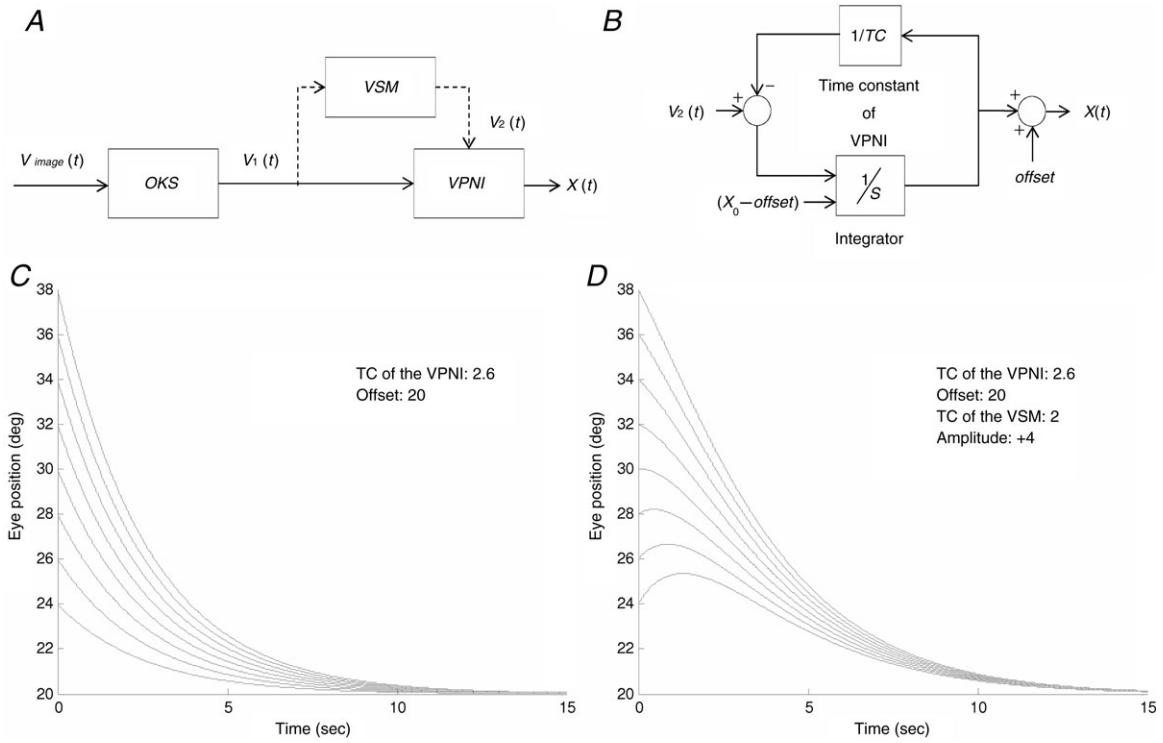

Figure 5. Conceptual model of larval ocular motor system, VPNI Simulink model and modelling results
A, conceptual model of larval ocular motor system. The optokinetic system (OKS) receives optokinetic signals $v_{image}(t)$ from the visual surround and sends eye velocity signals $v_1(t)$ to the velocity-to-position neural integrator (VPNI). The velocity storage mechanism (VSM) is charged by the velocity signal $v_1(t)$ from the OKS as well and sends velocity commands $v_2(t)$ to the VPNI. The VPNI then integrates the velocity commands into position signals $x(t)$. *B*, schematic plot of the VPNI model. The model receives velocity signals from the VSM and converts these signals into position commands. TC denotes the time constant of the VPNI, $v_2(t)$ denotes the velocity signal from the VSM, x_0 denotes initial eye position, 'offset' denotes final eye position, and $x(t)$ denotes eye displacement. *B*, simulated eye drifts without the VSM. *C*, simulated eye drifts with a stored velocity of an amplitude of 4 deg s^{-1} and a time constant of 2 s.

1973). In zebrafish larvae, the VPNI is not fully developed, i.e. the integrator is leaky, which leads to exponential centripetal drifts after each saccade (Fig. 4*B*). Note that this ocular drift only takes place in darkness. In the presence of a structured visual surround, postsaccadic eye positions are stable (Fig. 2*A*, middle). Thus, it appears that the optokinetic system is able to compensate for the leakiness of the VPNI by minimizing the retinal slip since the smooth pursuit system does not play a role in the afoveated zebrafish. Another consequence of VPNI leakiness is that slow-phase eye velocity during the OKR drops as the beating field of the eyes swiftly moves in the direction of the slow phase after the beginning of optokinetic stimulation. In this situation, the centripetal

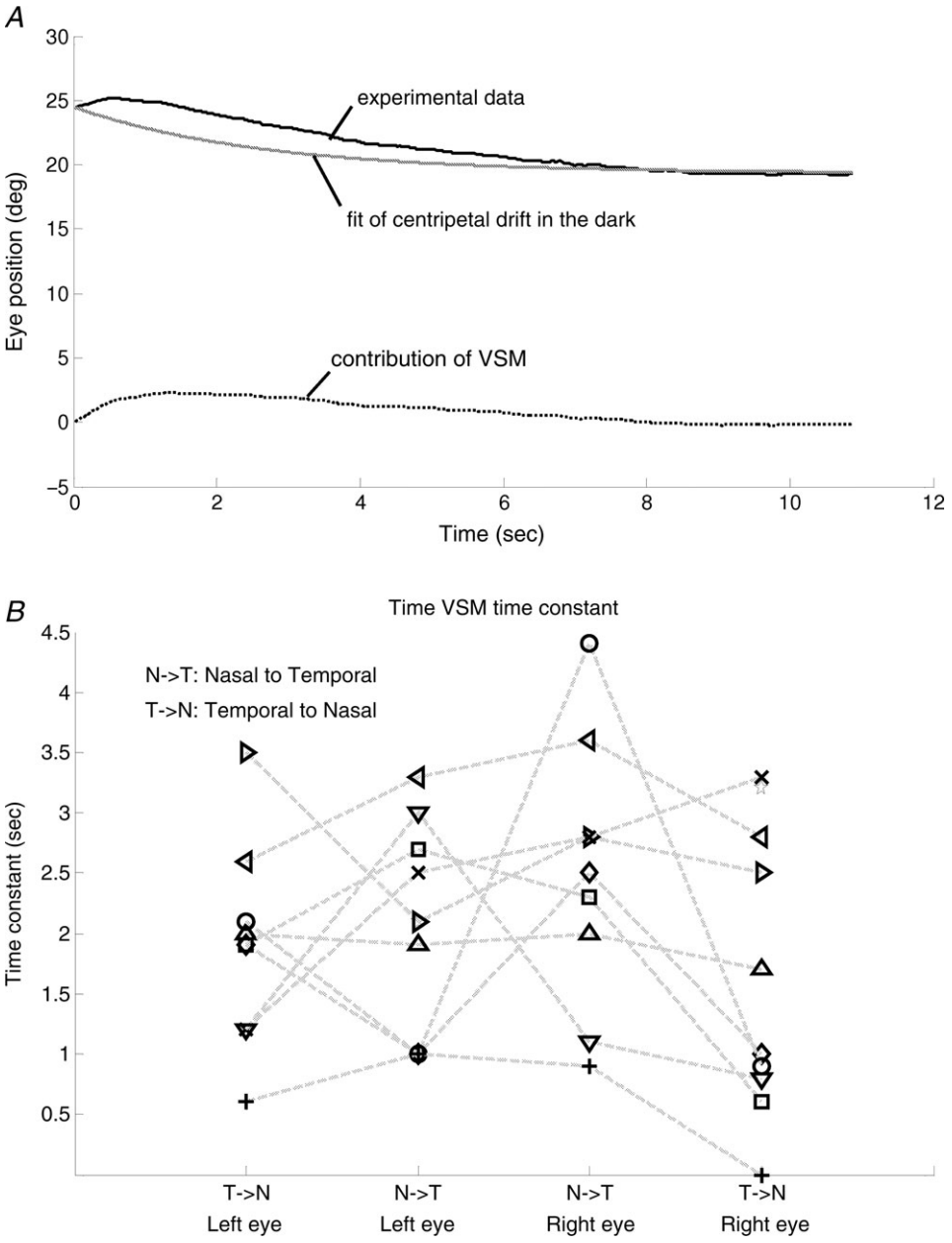

Figure 6. Estimation of time constant of the VSM
A, the black line represents the OKAR obtained from experimental data. The grey line represents predicted eye position from the analysis of drift behaviour in the dark. The dotted line represents the contribution of the VSM, used for computing the time constant of the VSM by iterative fitting. *B*, the estimated median time constants of the VSM of all larvae ($n = 10$). Note that one larva has only two time constants of the VPNI due to absence of eye movements in one direction (see Fig. 4*D*). In this case, the time constant of the VSM could not be estimated. Nine larvae had four values indicating the median time constant of two eyes in two directions. Values of each fish, except for the one with only two data points, are connected by a dashed line.

drift opposes the OKR, which decreases the net velocity (Fig. 3*B* and *D*).

Overall, zebrafish larvae have a well-developed OKR, an only rudimentarily developed VPNI, a still lacking horizontal aVOR, and – unexpectedly – a VSM. What could be the purpose of this VSM?

We conjecture that the VSM acts mainly to enhance the OKR, which could be beneficial for at least three different ocular motor aspects during optokinetic stimulation.

(1) Maintaining OKR velocity during stimulus interruptions. Maintaining the OKR in a natural environment under water, where illumination changes caused by surface wave reflection are very irregular, is critical for retinal stabilization in zebrafish. Such an irregular visual stimulus can also be induced by swimming behaviour. Thus, the VSM may function as a low pass filter to smooth brief velocity changes in the visual surround and/or working memory that stores velocity information of the visual surround for subsequent recovery of the OKR after interruptions of the visual stimulus. In other words, the stored velocity signal prevents the OKR from breaking down too quickly in the ever-changing visual surrounding.

(2) Maintaining OKR velocity during fast phases. Similarly, the VSM keeps the slow phase eye velocity relatively stable, although the optokinetic stimulus is repetitively interrupted during fast phases of nystagmus.

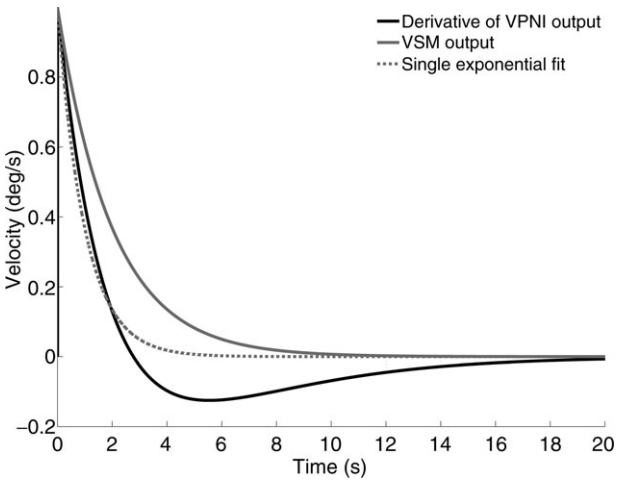

Figure 7. Simulations of the effect of VPNI on VSM output
The black line shows the derivative of the eye position obtained assuming that a leaky VPNI (time constant = 4 s) processes a negative exponential velocity input similar to the one generated by a VSM with a 2 s time constant during the OKAR (continuous grey line). The grey dotted line shows the best fit of the black line neglecting the role of the VPNI and fitting a single exponential function. The estimated time constant of the VSM is less than half that of the grey continuous line used to generate the black line. Using a lower VPNI time constant, similar to those we found in most of our larvae, would make the difference even more marked.

The time constant for the rise and fall of the OKR is estimated at about 350 ms while fast phases in larval zebrafish last around 500 ms (Fig. 3*B* and *D*). So without the VSM, OKR velocity would drop close to zero during each fast phase. The VSM thus allows eye velocity to stay close to the stimulus velocity after each saccade, without the need for a substantial 'build-up' period.

(3) Improving gaze stability before the emergence of a horizontal aVOR. Already at the larval stage (3–4 dpf) when beginning to swim upright, zebrafish display undulatory swimming in the horizontal plane with frequent head/body turns. With no functional horizontal aVOR at this stage, such swimming behaviour could substantially compromise gaze stability. The developmental advantage of a functional VSM at such an early stage could lie in the thus enhanced efficiency of the OKR that may help partially compensate for the absent aVOR and vastly improve gaze stability.

Relation between the VSM and the aVOR

It is generally thought that a functional VSM depends on the aVOR since unilateral labyrinthectomy shortens the VSM time constant and bilateral labyrinthectomy eliminates the VSM (Cohen *et al.* 1973; Raphan *et al.* 1979). Since the VSM also drives the OKAR, OKAR duration is shortened after unilateral labyrinthectomy and can no longer be elicited after bilateral labyrinthectomy (Cohen *et al.* 1973; Uemura & Cohen, 1973; Collewijn, 1976; Zee *et al.* 1976; Waespe & Wolfensberger, 1985).

Our data suggest that in zebrafish the VSM does not depend on angular vestibular input in early development since zebrafish larvae do not yet have a functional horizontal aVOR (Beck *et al.* 2004; Lambert *et al.* 2008). However, bilateral labyrinthectomy and/or section of the VIIIth nerves eliminate the VSM and the horizontal aVOR in adult animals (Cohen *et al.* 1973, 1983; Uemura & Cohen, 1973; Collewijn, 1976; Zee *et al.* 1976; Waespe & Wolfensberger, 1985), indicating that aVOR later becomes the dominant and possibly indispensable input to the VSM. Unfortunately, to our best knowledge, no systematic measurements of the OKAR after bilateral labyrinthectomy in fish exist. We hypothesize that, at a later stage when the semicircular canals become functional (horizontal aVOR detectible at 35 dpf; Beck *et al.* 2004), angular velocity signals from the labyrinths will gain access to the pre-existing VSM. The VSM may also receive angular velocity signals via a utricle-driven mechanism that interacts with visual input (Lauren & Angelaki, 2011; Bianco *et al.* 2012). The way in which vestibular and optokinetic signals interact to regulate the VSM is complex and needs further study as illustrated by selective abolishment of horizontal aVOR (i.e. horizontal

optokinetic after-nystagmus (OKAN) not affected) after canal plugging (Cohen *et al.* 1983). Taken together, if the early VSM found in the present study did not originate from optokinetic stimulation alone, semicircular canals may contribute to the early VSM either via the lateral semicircular canal nerves or by the canal afferents somehow superimposing rotation signals onto the functional otolith scaffold.

In order to verify the origin of the early development of a VSM without a canal-driven aVOR and the role of the OKR and aVOR in the development of the VSM, follow-up studies need to address the following question: how do early visual deprivation, and conversely, more-than-normal exposure to optokinetic stimulation, shape the VSM development? Moreover, a developmental study of the horizontal aVOR in relation to the development of the OKAR/OKAN is required.

Conclusion

The emergence of the VSM shortly after the manifestation of the OKR when larval zebrafish do not yet display a horizontal aVOR suggests that, at an early larval stage of zebrafish, the VSM may be regulated primarily by the OKR (i.e. the visual signal) to increase the efficacy of ocular motor control.

References

Abadi R & Pantazidou M (1997). Monocular optokinetic nystagmus in humans with age-related maculopathy. *Br J Ophthalmol* **81**, 123–129.

Angelaki DE & Cullen KE (2008). Vestibular system: The many facts of a multimodal sense. *Annu Rev Neurosci* **31**, 125–150.

Baarsma E & Collewijn H (1974). Vestibulo-ocular and optokinetic reactions to rotation and their interaction in the rabbit. *J Physiol* **238**, 603–625.

Beck JC, Gilland E, Tank DW & Baker R (2004). Quantifying the ontogeny of optokinetic and vestibuloocular behaviors in zebrafish, medaka, and goldfish. *J Neurophysiol* **92**, 3546–3561.

Bianco IH, Ma LH, Schoppik D, Robson DN, Orger MB, Beck JC, Li JM, Schier AF, Engert F & Baker R (2012). The tangential nucleus controls a gravito-inertial vestibulo-ocular reflex. *Curr Biol* **14**, 1285–1295.

Cohen B, Henn V, Raphan T & Dennett D (1981). Velocity storage, nystagmus, and visual-vestibular interactions in humans. *Ann N Y Acad Sci* **374**, 421–433.

Cohen B & Komatsuzaki A (1972). Eye movements induced by stimulation of the pontine reticular formation: evidence for integration in oculomotor pathways. *Exp Neurol* **36**, 101–117.

Cohen B, Matsuo V & Raphan T (1977). Quantitative analysis of the velocity characteristics of optokinetic nystagmus and optokinetic after-nystagmus. *J Physiol* **270**, 321–344.

Cohen B, Suzuki JI & Raphan T (1983). Role of the otolith organs in generation of horizontal nystagmus: effects of selective labyrinthine lesions. *Brain Res* **276**, 159–164.

Cohen B, Uemura T & Takemori S (1973). Effects of labyrinthectomy on optokinetic nystagmus (OKN) and optokinetic after-nystagmus (OKAN). *Int J Equilib Res* **3**, 80–93.

Collewijn H (1976). Impairment of optokinetic (after-)nystagmus by labyrinthectomy in the rabbit. *Exp Neurol* **52**, 146–156.

Easter SS Jr & Nicola GN (1997). The development of eye movements in the zebrafish (*Danio rerio*). *Dev Psychobiol* **31**, 267–276.

Haffter P, Granato M, Brand M, Mullins MC, Hammerschmidt M, Kane DA, Odenthal J, van Eeden FJ, Jiang YJ, Heisenberg CP, Kelsh RN, Furutani-Seiki M, Vogelsang E, Beuchle D, Schach U, Fabian C & Nusslein-Volhard C (1996). The identification of genes with unique and essential functions in the development of the zebrafish, *Danio rerio*. *Development* **123**, 1–36.

Hess BJM, Prechta W, Reber A & Cazin L (1985). Horizontal optokinetic ocular nystagmus in the pigmented rat. *Neuroscience* **15**, 97–107.

Honrubia V, Downey WL, Mitchell DP & Ward PH (1968). Experimental studies on optokinetic nystagmus II. Normal Humans. *Acta Otolaryngol* **65**, 441–448.

Huang YY & Neuhauss SC (2008). The optokinetic response in zebrafish and its applications. *Front Biosci* **13**, 1899–1916.

Igarashi M, Takahashi M & Homick JL (1977). Optokinetic nystagmus and vestibular stimulation in squirrel monkey model. *Arch Otorhinolaryngol* **218**, 115–121.

Lambert FM, Beck JC, Baker R & Straka H (2008). Semicircular canal size determines the developmental onset of angular vestibuloocular reflexes in larval *Xenopus*. *J Neurosci* **32**, 8086–8095.

Laurens J & Angelaki DE (2011). The functional significance of velocity storage and its dependence on gravity. *Exp Brain Res* **210**, 407–422.

Miri A, Daie K, Arrenberg AB, Baier H, Aksay E & Tank DW (2011). Spatial gradients and multidimensional dynamics in a neural integrator circuit. *Nat Neurosci* **14**, 1150–1159.

Mo W, Chen F, Nechiporuk A & Nicolson T (2010). Quantification of vestibular-induced eye movements in zebrafish larvae. *BMC Neurosci* **11**, 110.

Mullins MC, Hammerschmidt M, Haffter P & Nusslein-Volhard C (1994). Large-scale mutagenesis in the zebrafish: in search of genes controlling development in a vertebrate. *Curr Biol* **4**, 189–202.

Paige GD (1983). Vestibuloocular reflex and its interactions with visual following mechanisms in the squirrel monkey. I. Response characteristics in normal animals. *J Neurophysiol* **49**, 134–151.

Ramat S & Bertolini G (2009). Estimating the Time Constants of the rVOR. *Ann NY Acad Sci* **1164**, 140–146.

Raphan T, Cohen B & Matsuo V (1977). A velocity-storage mechanism responsible for optokinetic nystagmus (OKN), optokinetic after-nystagmus (OKAN) and vestibular nystagmus. In *Control of Gaze by Brain Stem Neurons, Developments in Neuroscience*, vol. 1, ed. Baker R & Berthoz A, pp. 37–47. Elsevier/North-Holland Biomedical Press, Amsterdam.

Raphan T, Matsuo V & Cohen B (1979). Velocity storage in the vestibuloocular reflex arc (VOR). *Exp Brain Res* **35**, 229–248.

Robinson DA (1964). The mechanics of human saccadic eye movement. *J Physiol* **174**, 245–264.
Robinson DA (1977). Linear addition of optokinetic and vestibular signals in the vestibular nucleus. *Exp Brain Res* **30**, 447–450.
Robinson DA (1981). The use of control systems analysis in the neurophysiology of eye movements. *Annu Rev Neurosci* **4**, 463–503.
Schweigart G, Mergner T, Evdokimidis I, Morand S & Becker W (1997). Gaze stabilization by optokinetic reflex (OKR) and vestibulo-ocular reflex (VOR) during active head rotation in man. *Vision Res* **37**, 1643–1652.
Sirkin DW, Hess BJM & Precht W (1985). Optokinetic nystagmus in albino rats depends on stimulus pattern. *Exp Brain Res* **61**, 218–221.
Skavenski AA & Robinson DA (1973). Role of abducens neurons in vestibuloocular reflex. *J Neurophysiol* **36**, 724–738.
Takahashi M & Igarashi M (1977). Comparison of vertical and horizontal optokinetic nystagmus in the squirrel monkey. *ORL J Otorhinolaryngol Relat Spec* **39**, 321–329.
Tan HS, Collewijn H & van der Steen J (1992). Optokinetic nystagmus in the rabbit and its modulation by bilateral microinjection of carbachol in the cerebellar flocculus. *Exp Brain Res* **90**, 456–468.
Tan HS, van der Steen J, Simpson JI & Collewijn H (1993). Three-dimensional organization of optokinetic response in the rabbit. *J Neurophysiol* **69**, 303–317.
Uemura T & Cohen B (1973). Effects of vestibular nuclei lesions on vestibulo-ocular reflexes and posture in monkeys. *Acta Otolaryngol Suppl* **315**, 1–71.
Waespe W & Henn V (1977). Vestibular nuclei activity during optokinetic after-nystagmus (OKAN) in the alert monkey. *Exp Brain Res* **30**, 323–330.
Waespe W & Wolfensberger M (1985). Optokinetic nystagmus (OKN) and optokinetic after-responses after bilateral vestibular neurectomy in the monkey. *Exp Brain Res* **60**, 263–269.
Zee D, Yee RD & Robinson DA (1976). Optokinetic responses in labyrinthine-defective human beings. *Brain Res* **113**, 423–428.

Additional information

Competing interests

None declared.

Author contributions

D.S., C.-C.C. and M.Y.-Y.H. conceived the study. C.-C.C. performed the experiments. C.-C.C., D.S., C.J.B., G.B., I.O. and M.Y.-Y.H. analysed the data. The research was conducted at the University Hospital Zurich, Switzerland. C.-C.C. and G.B. prepared the figures. D.S., C.-C.C. and M.Y.-Y.H. drafted the article and wrote the final paper with contributions from C.J.B., G.B., I.O. and K.P.W. All authors approved the final version of the paper. Fish were provided by S.C.F.N. who commented on the draft.

Funding

This work was supported by the Swiss National Science Foundation (SNF) grants PMPDP3_139754 (Marie Heim-Vögtlin programme) and 31003A-118069, Zurich Center for Integrative Human Physiology (ZIHP), and the Betty and David Koetser Foundation for Brain Research.

Acknowledgements

The authors would like to thank Dr Bernhard Hess for valuable conceptual input and discussions, the reviewers for their critical comments, Marco Penner for technical assistance, and Kara Dannenhauer for fish care.